

Towards a realistic prediction of catalyst durability from liquid half-cell tests

Timo Imhof,^{a,*} Roberta K. F. Della Bella,^b Björn M. Stühmeier,^b Hubert A. Gasteiger^b and Marc Ledendecker^{a,c,*}

^a Technical University of Darmstadt, Alarich-Weiss Strasse 10, 64287 Darmstadt

^b Technical University of Munich, Lichtenbergstrasse 4, 85748 Garching

^c Technical University of Munich, Schulgasse 22, 94315 Straubing

Supporting information

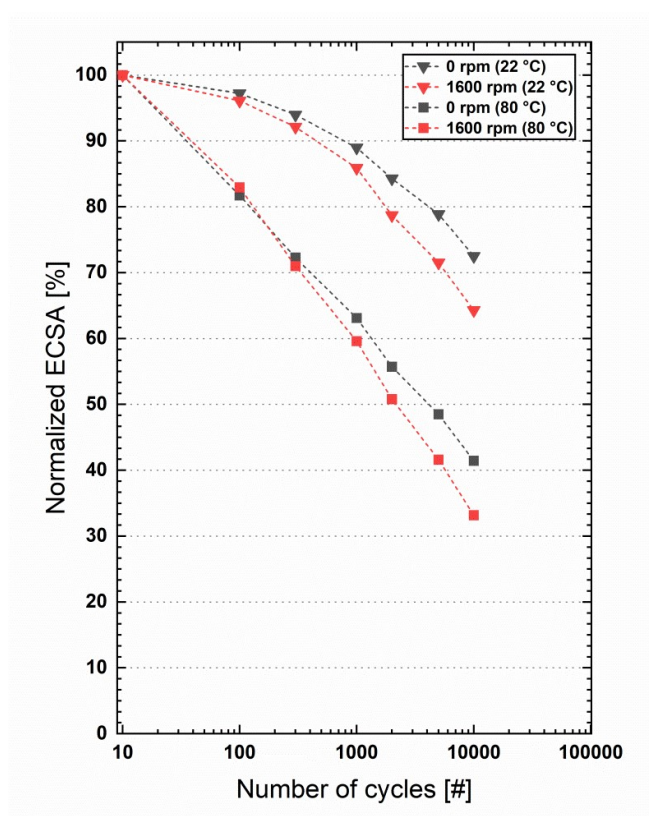


Figure S1: Normalized ECSA plotted against the number of aging cycles of RDE-based voltage cycling AST measurements (0.6/1.0 V_{RHE} square-waves with 1 s holds) at 22 or 80 °C, conducted at either 1,600 rpm or without rotation. Films of the 19.8 wt.% Pt/Vu catalyst where prepared with an I/C ratio of 0.1.

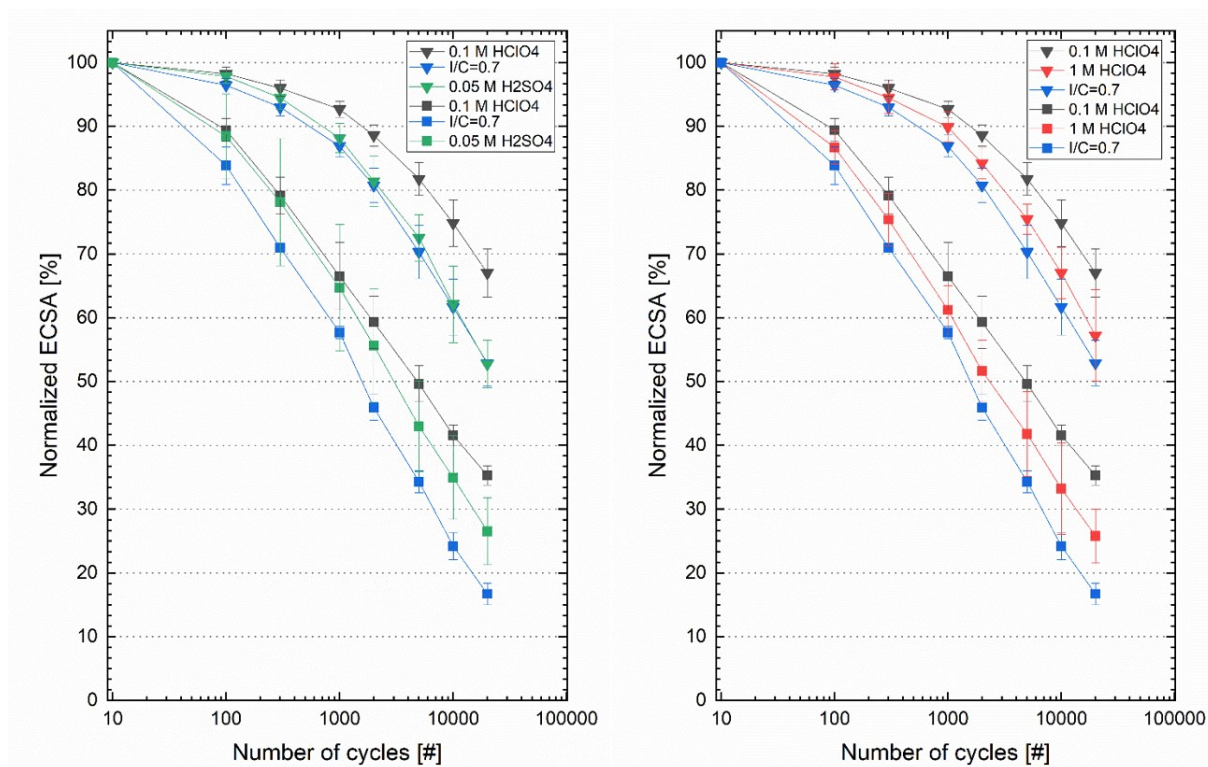


Figure S2: Normalized ECSA plotted against the number of aging cycles of RDE-based voltage cycling AST measurements (0.6/1.0 V_{RHE} square-waves with 1 s holds; at 0 rpm) at 22 °C (triangles) and 80 °C (squares), conducted in 0.05 M H_2SO_4 (left plot) and 1.0 M $HClO_4$ (right plot) for 19.8 wt.% Pt/Vu catalyst films without ionomer in comparison to measurements in 0.1 M $HClO_4$ with and without ionomer (blue lines named I/C=0.7).

Table S1: Measured pH values of the used electrolytes at room temperature and at 80 °C.

	measured pH	
	22 °C	80 °C
0.1 M $HClO_4$	1.10	1.10
0.05 M H_2SO_4	1.32	1.00
1 M $HClO_4$	0.45	0.07

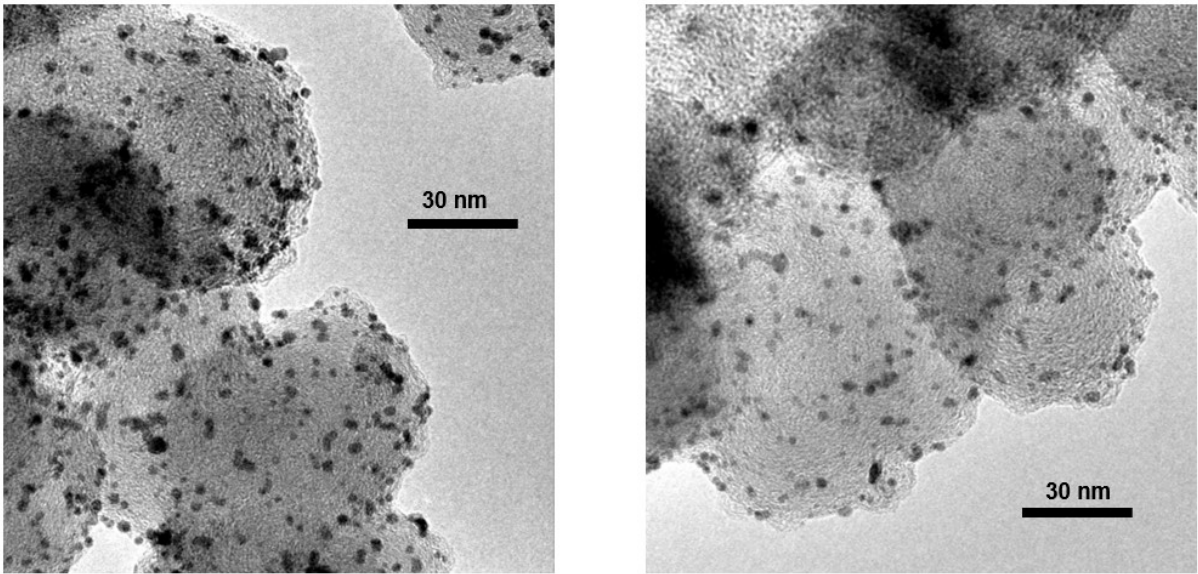


Figure S3: TEM images of the pristine 19.8 wt.% Pt/Vu catalyst.

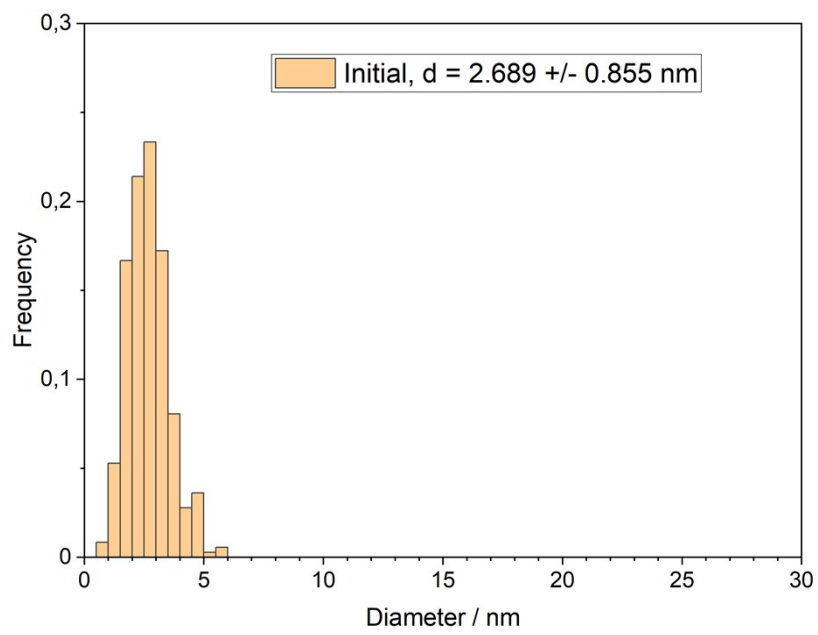


Figure S4: Particle size distribution of the pristine 19.8 wt.% Pt/Vu catalyst. The Sauter diameter calculated from the individual particle diameters is 3.2 nm.

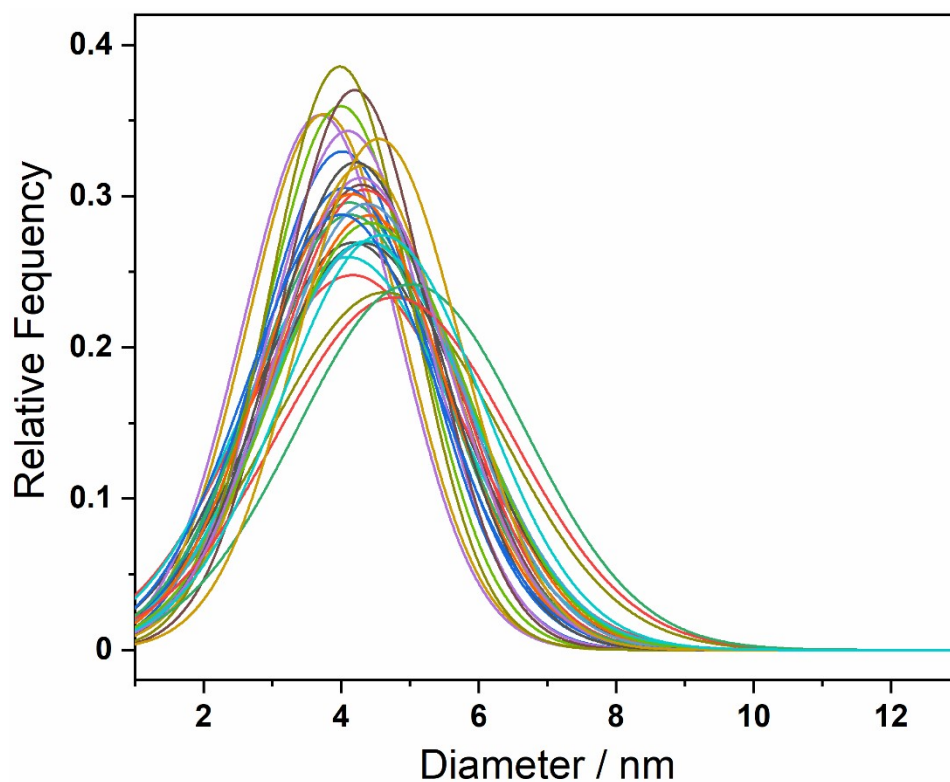


Figure S5: Particle size distributions of 34 individual carbon particles or aggregates of two samples after 100k AST cycles (0.6/1.0 V_{RHE} square-waves with 1 s holds) at room temperature in the RDE configuration (at 0 rpm).

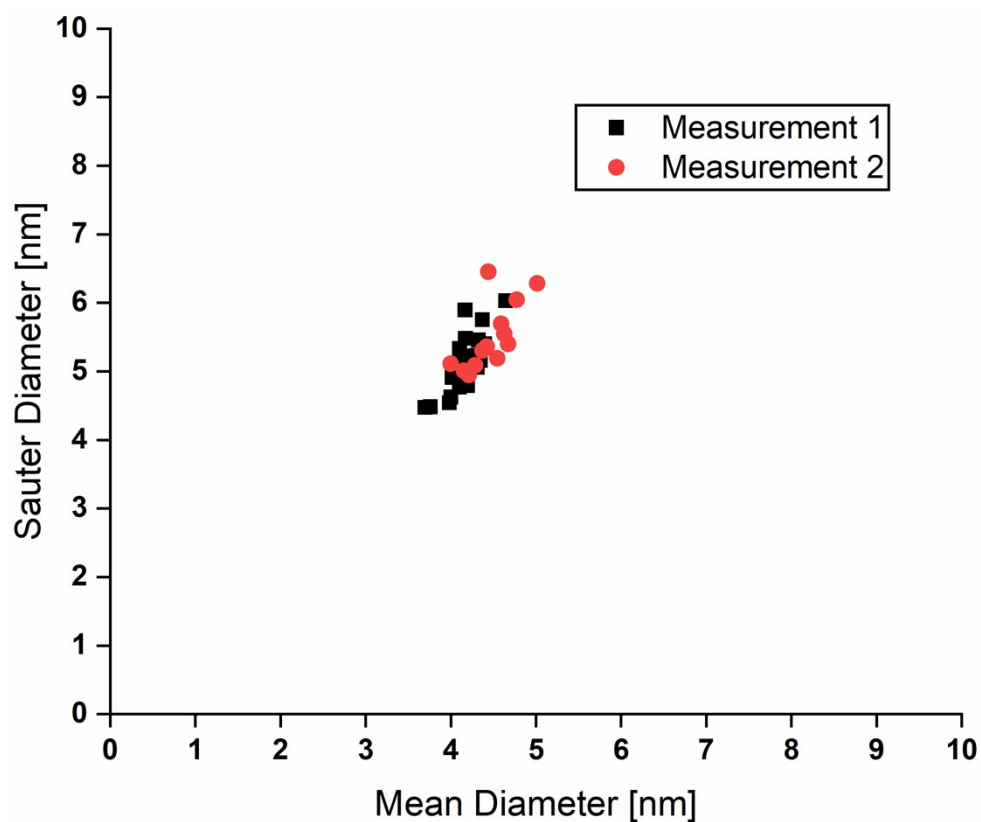


Figure S6: Sauter diameters plotted against the corresponding Pt mean diameters located on different individual carbon particles or aggregates of two samples taken from individual measurements after 100k AST cycles (0.6/1.0 V_{RHE} square-waves with 1 s holds) at room temperature in the RDE configuration (at 0 rpm).

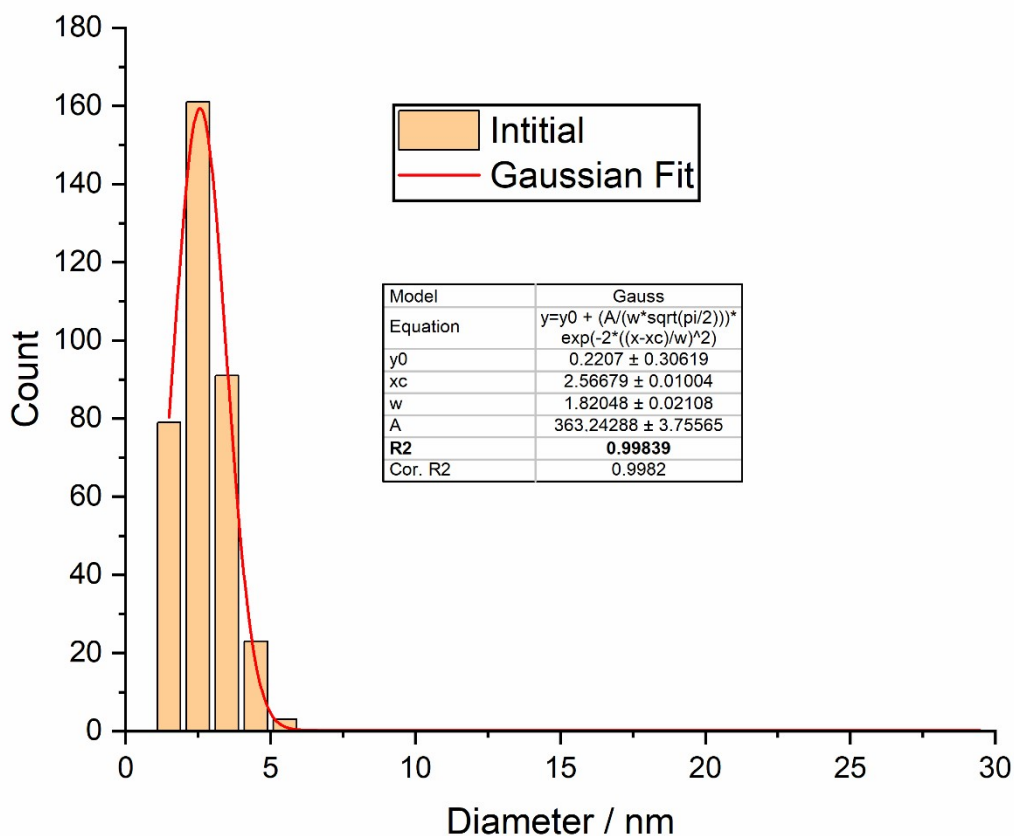


Figure S7: Gaussian fit of the PSD of the pristine 19.8 wt.% Pt/Vu catalyst.

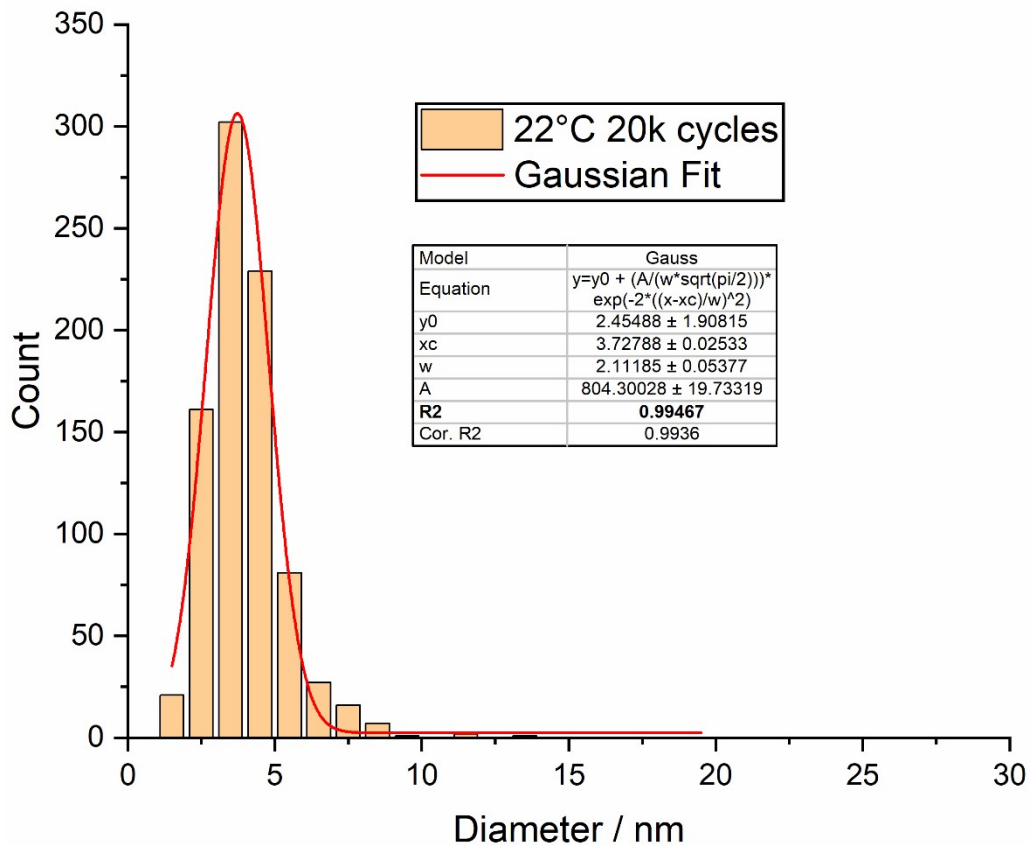


Figure S8: Gaussian fit of the PSD after 20k aging cycles (0.6/1.0 V_{RHE} square-waves with 1 s holds in the RDE configuration at 0 rpm) at room temperature for 19.8 wt.% Pt/Vu catalyst films without ionomer.

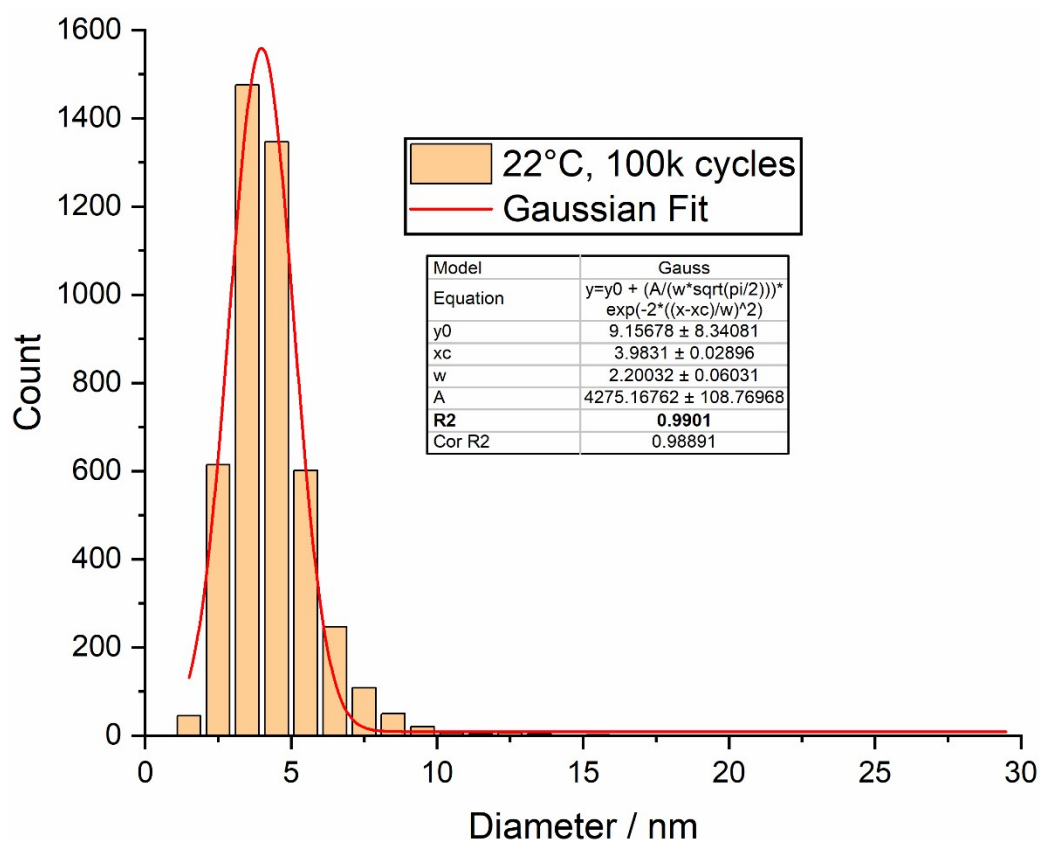


Figure S9: Gaussian fit of the PSD after 100k aging cycles (0.6/1.0 V_{RHE} square-waves with 1 s holds in the RDE configuration at 0 rpm) at room temperature for 19.8 wt.% Pt/Vu films without ionomer.

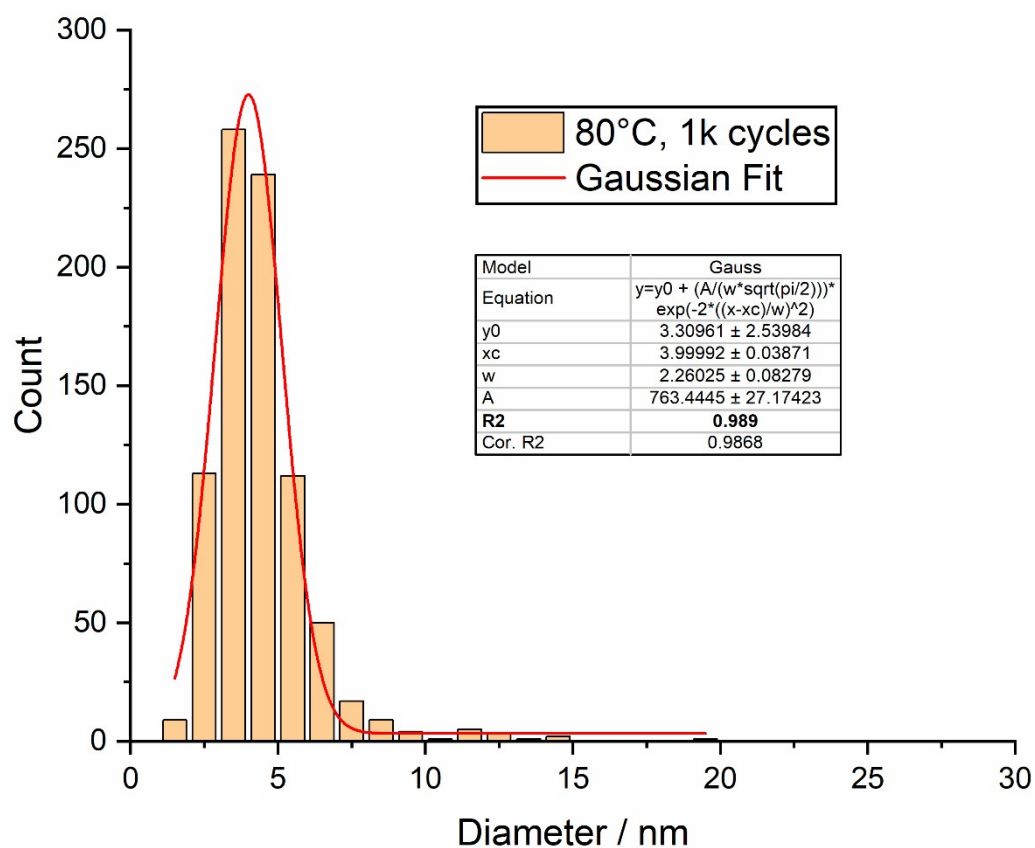


Figure S10: Gaussian fit of the PSD after 1k aging cycles (0.6/1.0 V_{RHE} square-waves with 1 s holds in the RDE configuration at 0 rpm) at 80 °C for 19.8 wt.% Pt/Vu films without ionomer.

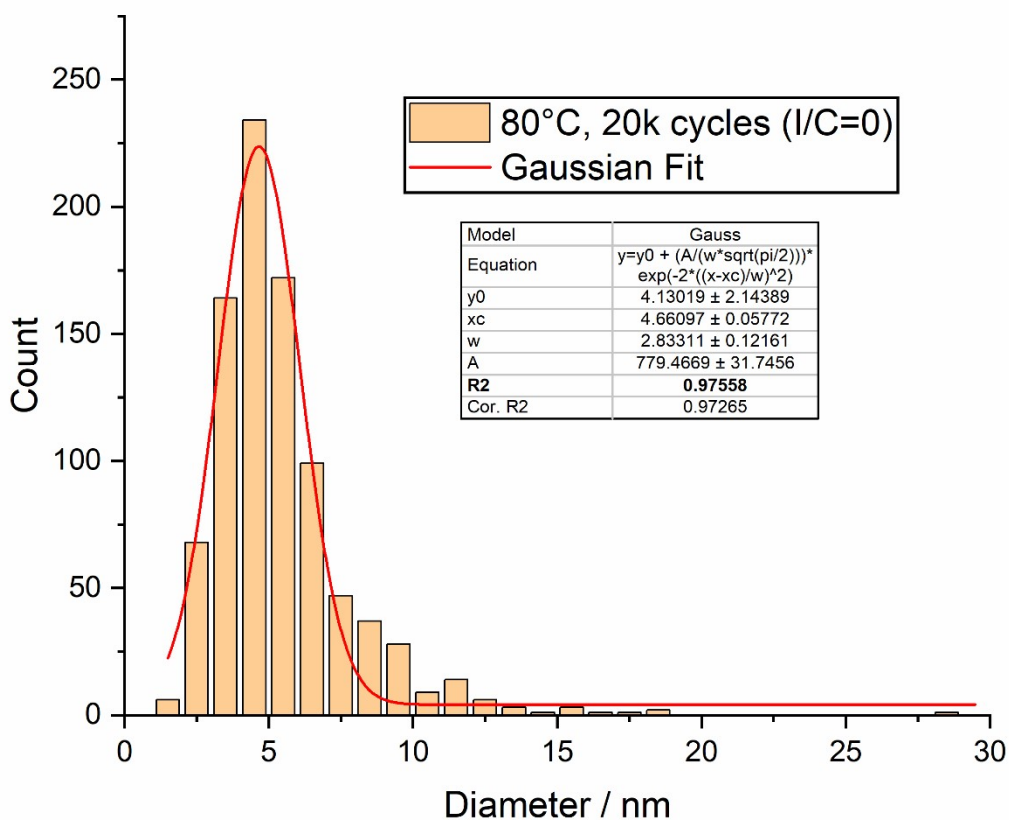


Figure S11: Gaussian fit of the PSD after 20k aging cycles (0.6/1.0 V_{RHE} square-waves with 1 s holds in the RDE configuration at 0 rpm) at 80 °C for 19.8 wt.% Pt/Vu films without ionomer.

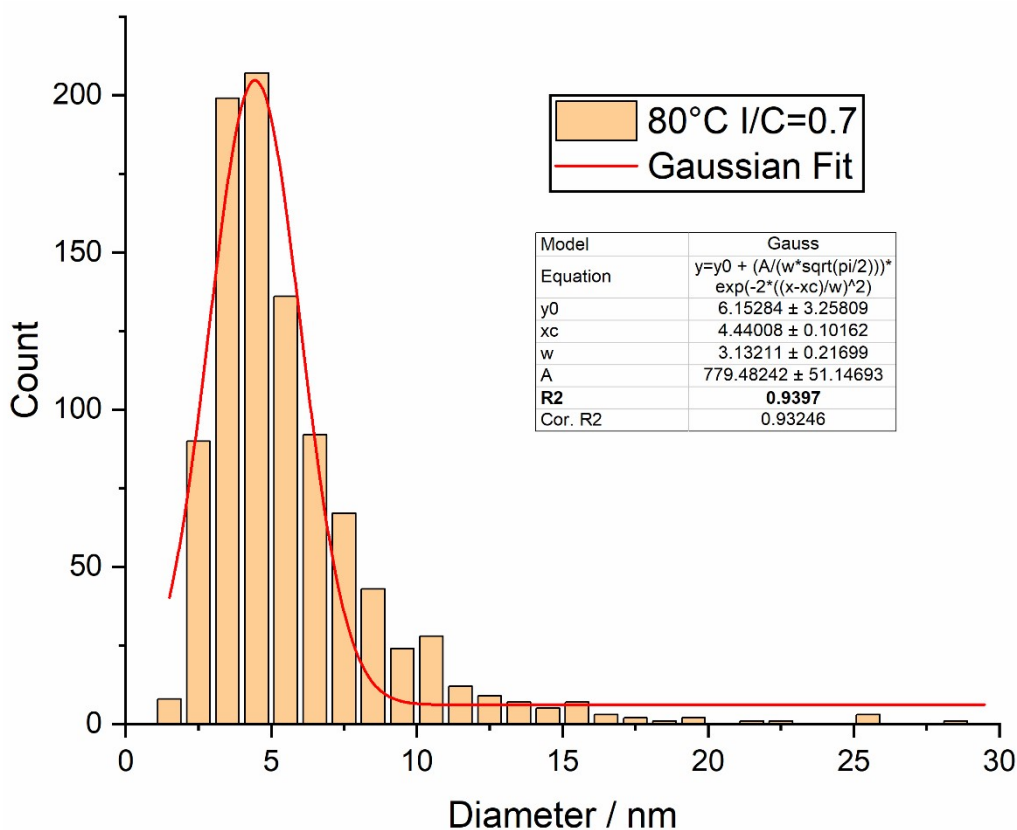


Figure S12: Gaussian fit of the PSD after 20k aging cycles (0.6/1.0 V_{RHE} square-waves with 1 s holds in the RDE configuration at 0 rpm) at 80 °C for 19.8 wt.% Pt/Vu films with ionomer.

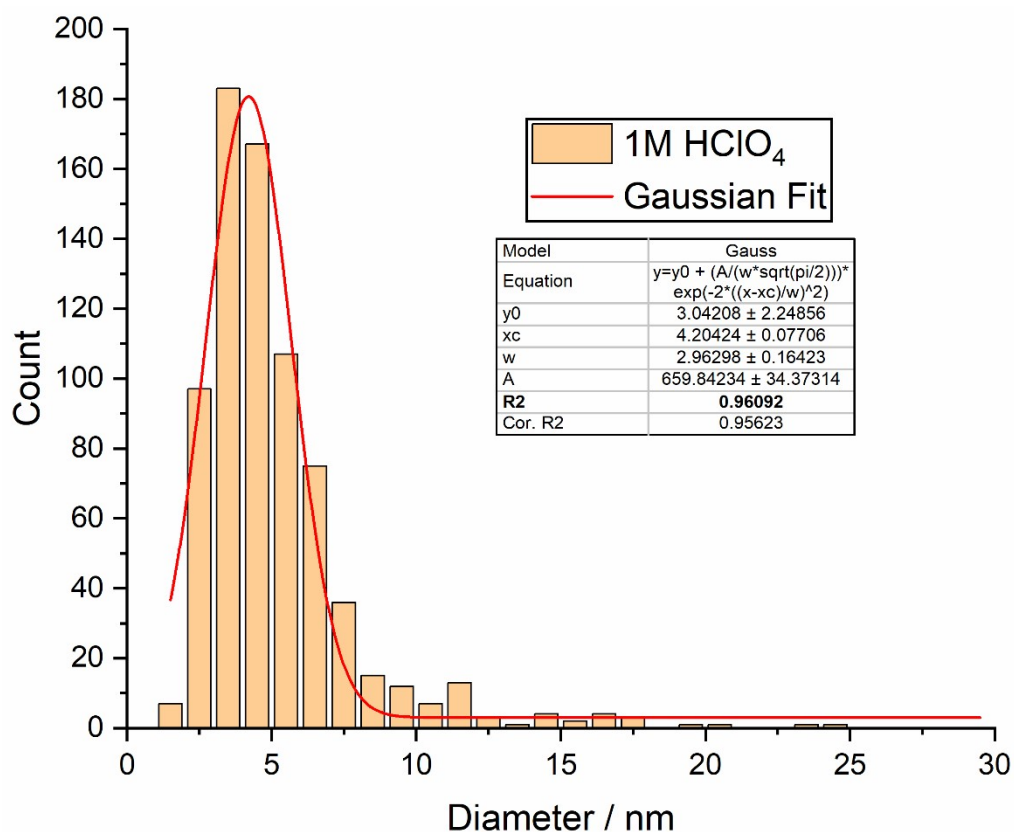


Figure S13: Gaussian fit of the PSD after 20k aging cycles (0.6/1.0 V_{RHE} square-waves with 1 s holds in the RDE configuration at 0 rpm) at 80 °C in 1 M $HClO_4$ for 19.8 wt.% Pt/Vu films without ionomer.

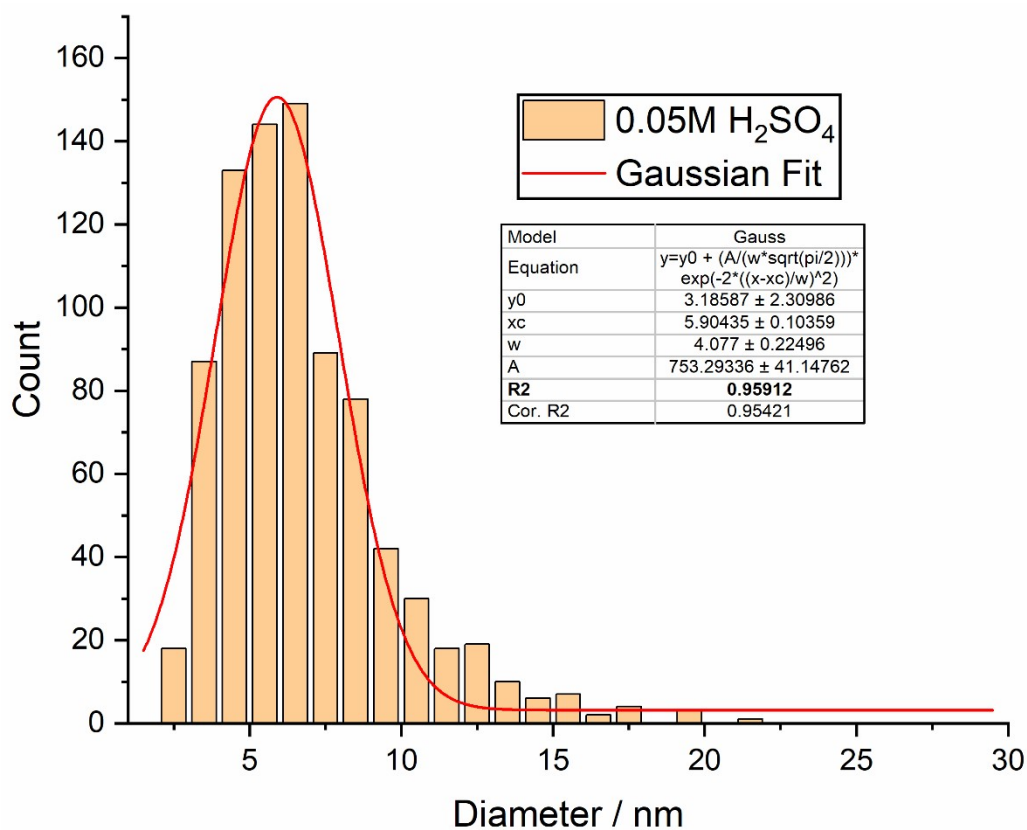


Figure S14: Gaussian fit of the PSD after 20k aging cycles (0.6/1.0 V_{RHE} square-waves with 1 s holds in the RDE configuration at 0 rpm) at 80 °C in 0.05 H_2SO_4 for 19.8 wt.% Pt/Vu films without ionomer.

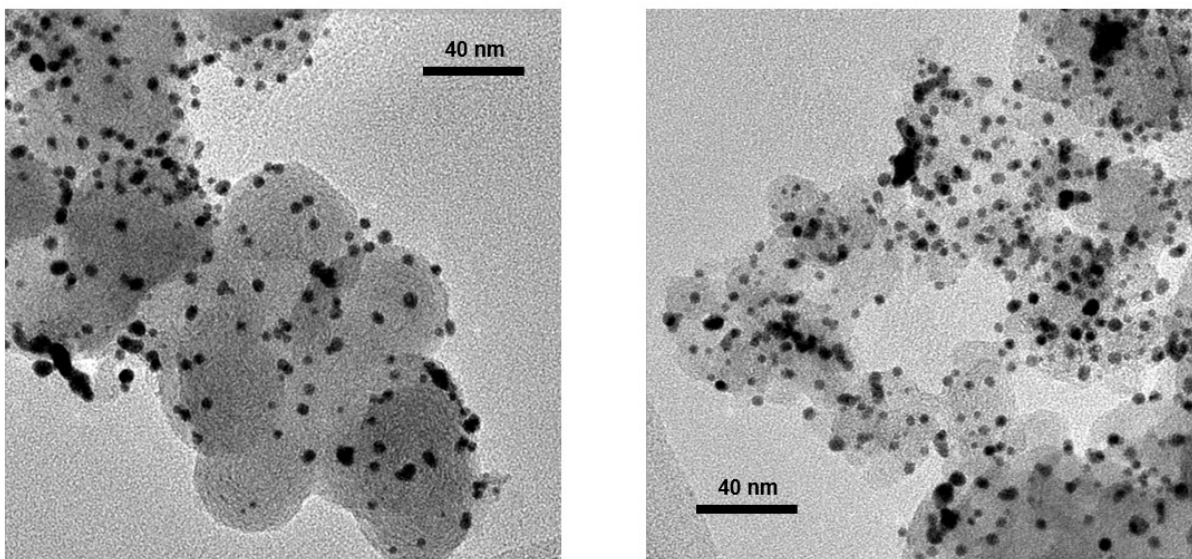


Figure S15: TEM images of degraded 19.8 wt.% Pt/Vu at 22 °C after 20k degradation cycles with a remaining ECSA of 67 % (refers to Figure 3 and 4).

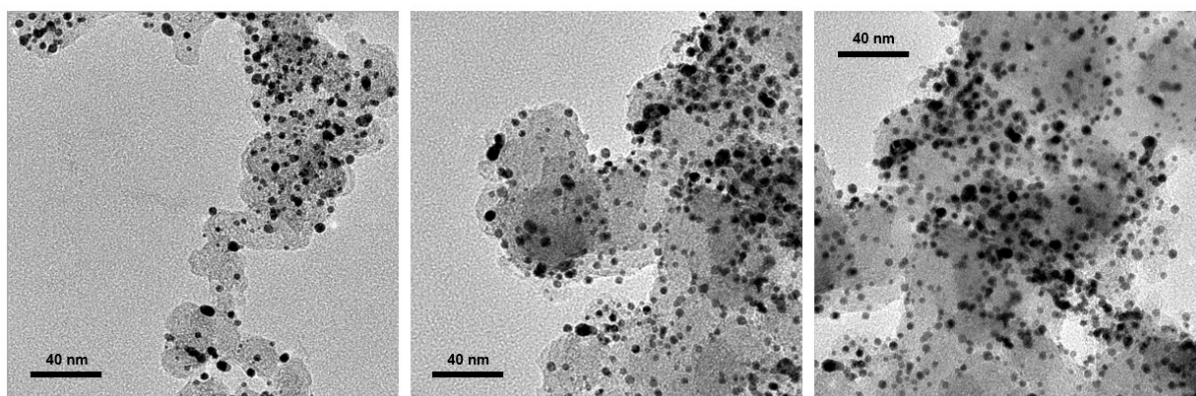


Figure S16 TEM images of degraded Pt/Vulcan at 80 °C after 1k degradation cycles with a remaining ECSA of 67 % (refers to Figure 3 and 4).

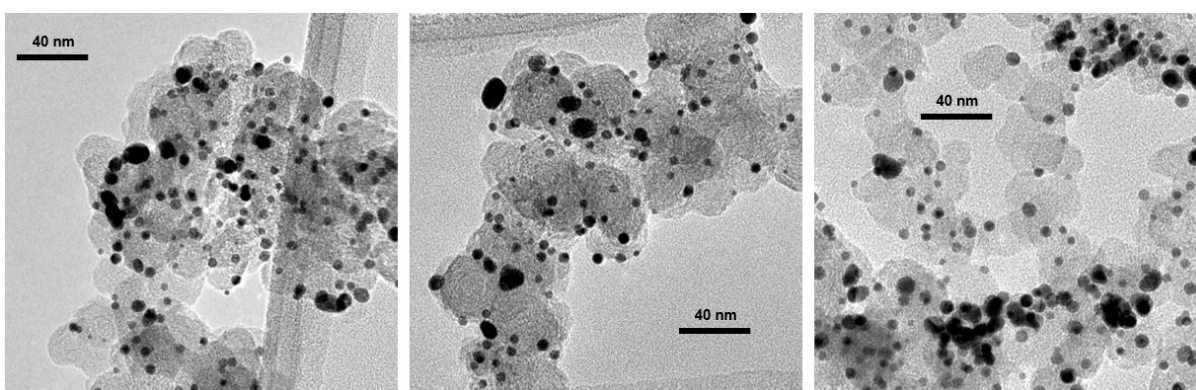


Figure S17: TEM images of a degraded Pt/Vulcan catalyst film without Nafion® at 80°C after 20k degradation cycles with a remaining ECSA of 35 % (refers to Figure 4 and 5).

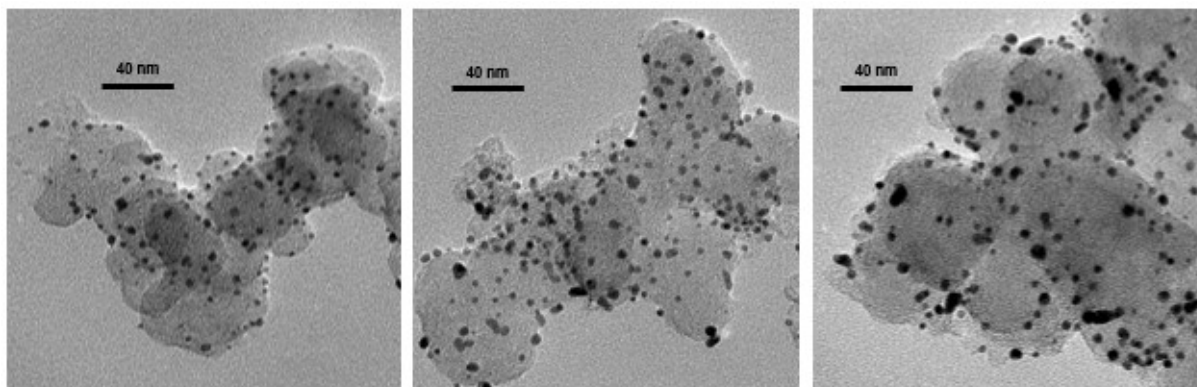


Figure S18: TEM images of degraded 19.8 wt.% Pt/Vu at 22 °C after 100k degradation cycles with a remaining ECSA of 38 % (refers to Figure 3 and 4).

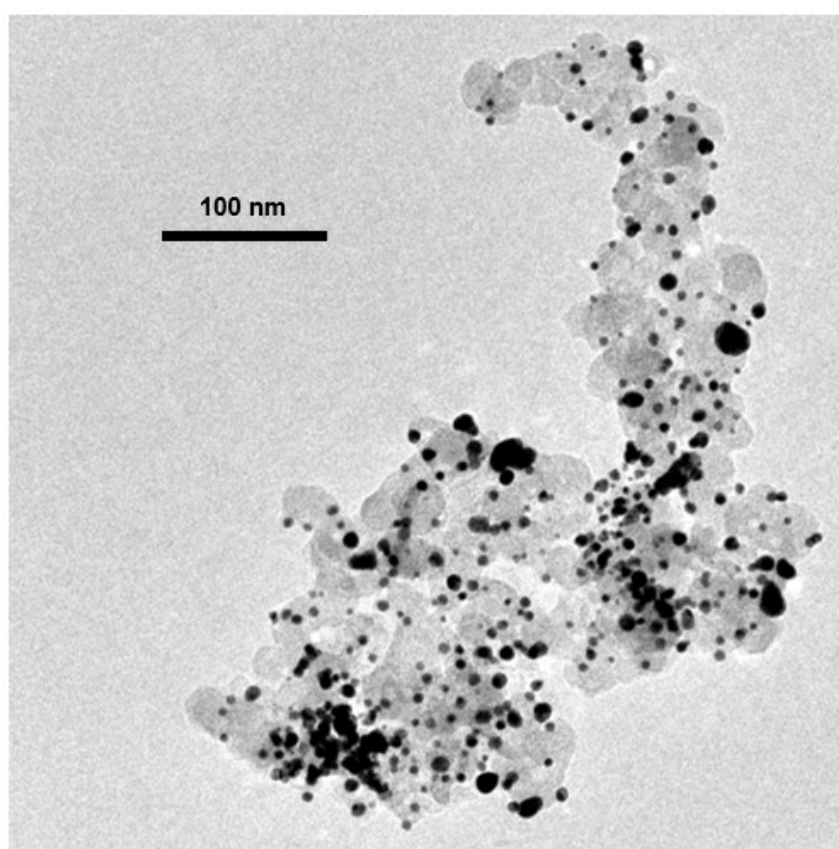


Figure S19: TEM image of a degraded Pt/Vulcan catalyst film with Nafion® ($I/C=0.7$) at 80°C after 20k degradation cycles with a remaining ECSA of 17 % (refers to Figure 5 and 6).

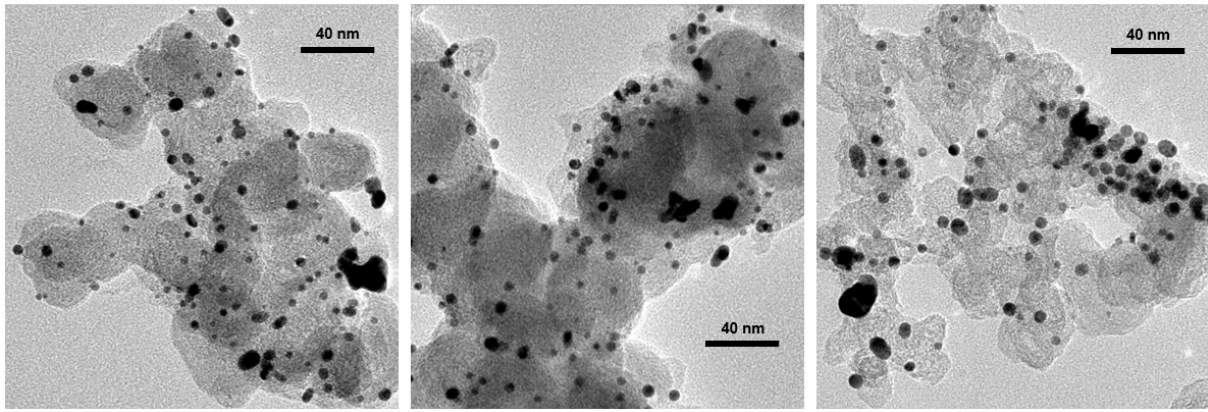


Figure S20: TEM images of a degraded Pt/Vulcan catalyst film without Nafion® in 1 M HClO₄ at 80°C after 20k degradation cycles with a remaining ECSA of 26 % (refers to Figure 7).

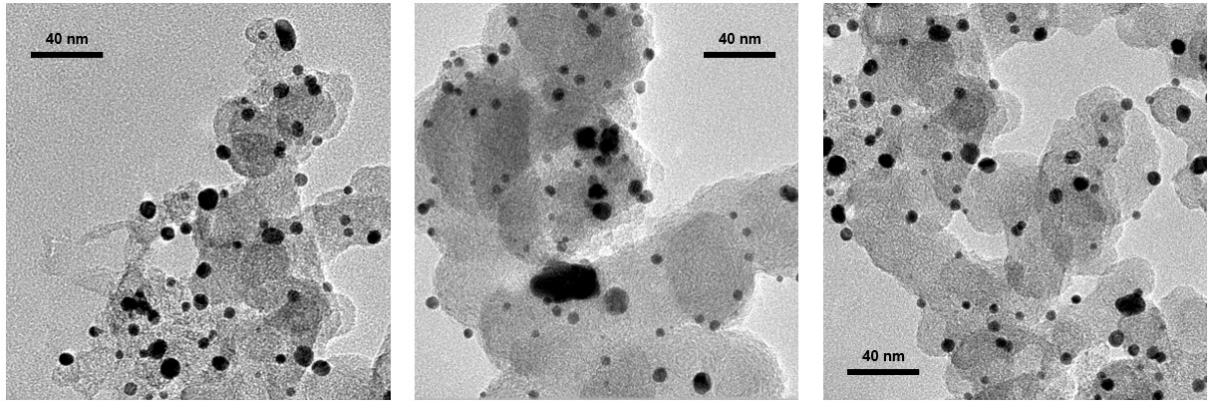


Figure S21: TEM images of a degraded Pt/Vulcan catalyst film without Nafion® in 0.05 M H₂SO₄ at 80°C after 20k degradation cycles with a remaining ECSA of 26 % (refers to Figure 7).

Table S2: Calculation of the proton concentration in fully hydrated Nafion®

Proton concentration in wet Nafion:	
EW of 1000	1000 g _{PFSA} /mol _{SO₃H} (EW of 1000)
Density (dry polymer)	2 g _{PFSA} /cm ³ _{PFSA} (dry polymer)
lambda value in liquid water	500 cm ³ _{PFSA} /mol _{SO₃H}
mass (water of hydration)	22
volume (water of hydration)	396 g _{H₂O} per mol _{SO₃H}
volume of fully hydrated Nafion	396 cm ³ _{H₂O} per mol _{SO₃H}
c (-SO ₃ H)	896 cm ³ _{H₂O+PFSA} per mol _{SO₃H}
c (H ⁺)	1.1 mol _{SO₃H} /l _{PFSA+H₂O}
	1.1 mol_{H⁺}/l_{PFSA+H₂O} for a super-acid

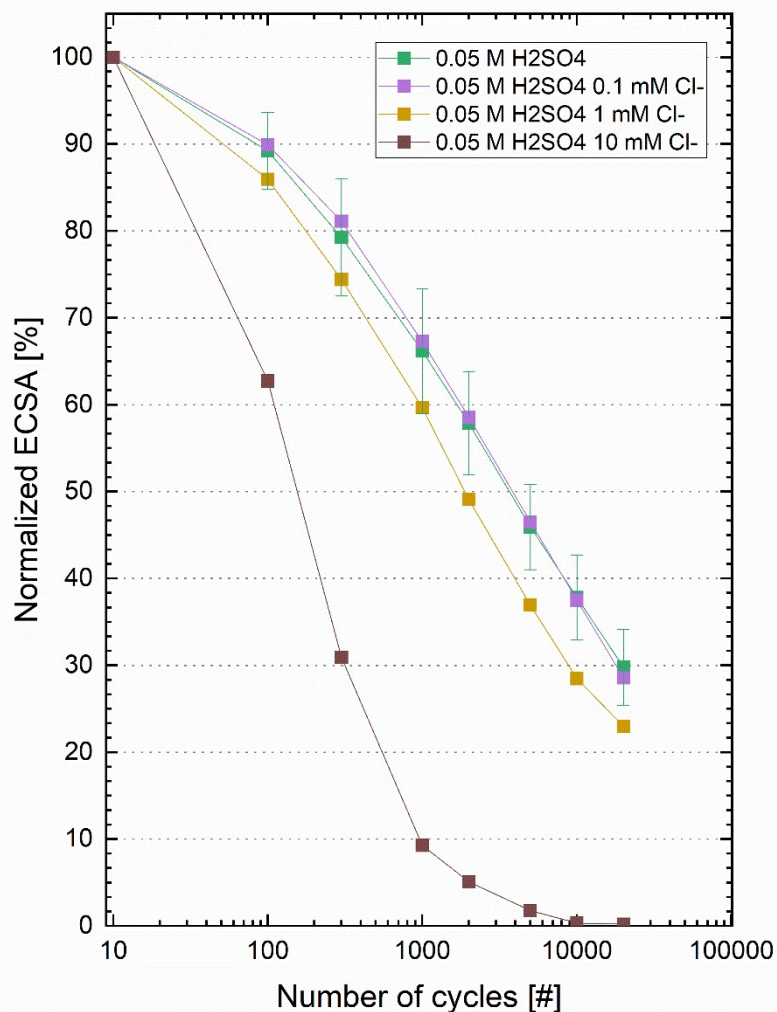


Figure S22: Normalized ECSA plotted against the number of aging cycles of RDE-based voltage cycling AST measurements (0.6/1.0 V_{RHE} square-waves with 1 s holds; at 0 rpm) at 80 °C, conducted in 0.05 M H_2SO_4 for 19.8 wt.% Pt/Vu catalyst films without ionomer and different concentrations of chloride ions 0.1 mM, 1 mM and 10 mM in the electrolyte.

The experiments with chloride impurities added to sulfuric acid electrolyte to simulate the possible degradation of the perchloric acid electrolyte at 80 °C depicted in Figure S22 show, that an increasing chloride concentration accelerates the ECSA loss upon AST cycling. On the other hand, this effect is only measurable at sufficiently high concentrations of ≥ 1 mM Cl⁻. For experiments conducted in 0.1 M HClO₄ electrolyte, we don't expect chlorine formed by the degradation of perchlorate to influence the degradation, as in these experiments, the ECSA loss was even smaller than in 0.05 M sulphuric acid (ref. Figure 7). ASTs conducted in 0.5 M H_2SO_4 showed higher ECSA loss than in 0.05 M H_2SO_4 (see Figure S23), similar to the comparison of 0.1 M and 1 M HClO₄ (ref. Figure 7). Hence, we conclude that the formation of chlorine from perchlorate degradation is still not sufficient in 1 M HClO₄ to significantly influence the measured ECSA loss, although it cannot be excluded with certainty due to lower perchloric acid stability at higher concentrations.¹

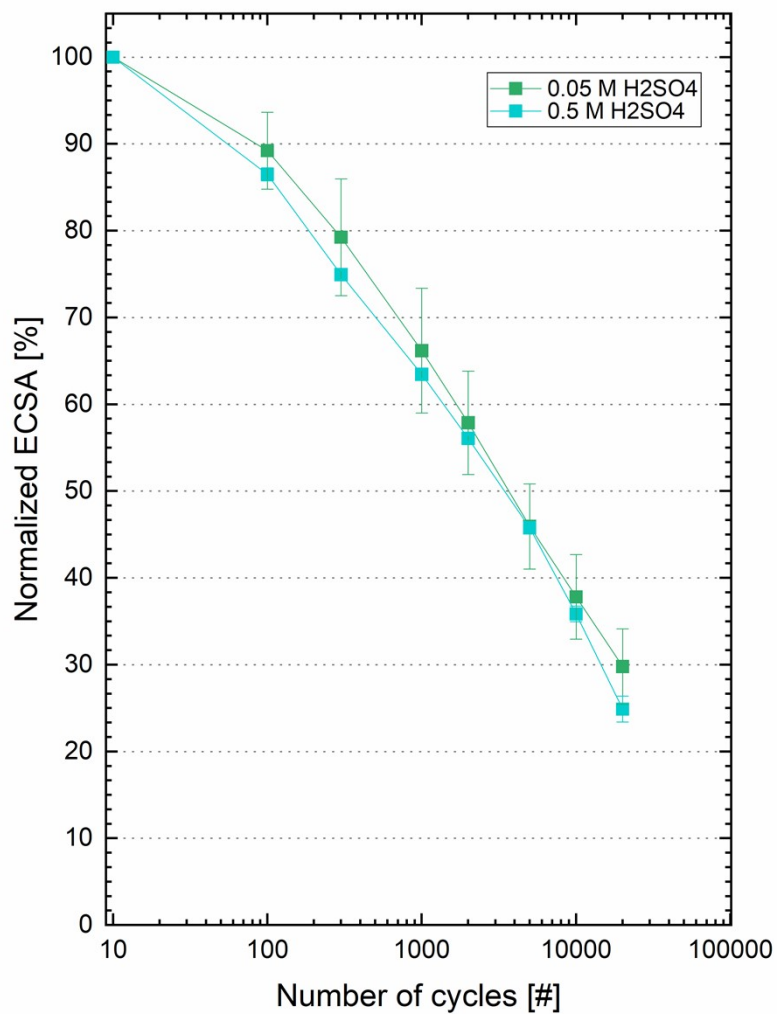


Figure S 23: Normalized ECSA plotted against the number of aging cycles of RDE-based voltage cycling AST measurements (0.6/1.0 V_{RHE} square-waves with 1 s holds; at 0 rpm) at 80 °C, conducted in 0.05 M and 0.5 M H_2SO_4 for 19.8 wt.% Pt/Vu catalyst films.

1 F. Solymosi, *Acta Phys. Chem.*, 1977, **23**, 317–354.